

# Whole-Body Vibration Induces Pain and Lumbar Spinal Inflammation Responses in the Rat That Vary With the Vibration Profile

Martha E. Zeeman, Sonia Kartha, Beth A. Winkelstein

Department of Bioengineering, University of Pennsylvania, 240 Skirkanich Hall, 210 S. 33rd St, Philadelphia, Pennsylvania 19104-6321

Received 16 January 2016; accepted 23 March 2016

Published online 13 April 2016 in Wiley Online Library (wileyonlinelibrary.com). DOI 10.1002/jor.23243

**ABSTRACT:** Whole-body vibration (WBV) is linked epidemiologically to neck and back pain in humans, and to forepaw mechanical allodynia and cervical neuroinflammation in a rodent model of WBV, but the response of the low back and lumbar spine to WBV is unknown. A rat model of WBV was used to determine the effect of different WBV exposures on hind paw behavioral sensitivity and neuroinflammation in the lumbar spinal cord. Rats were exposed to 30 min of WBV at either 8 or 15 Hz on days 0 and 7, with the lumbar spinal cord assayed using immunohistochemistry at day 14. Behavioral sensitivity was measured using mechanical stimulation of the hind paws to determine the onset, persistence, and/or recovery of allodynia. Both WBV exposures induce mechanical allodynia 1 day following WBV, but only the 8 Hz WBV induces a sustained decrease in the withdrawal threshold through day 14. Similarly, increased activation of microglia, macrophages, and astrocytes in the superficial dorsal horn of the lumbar spinal cord is only evident after the painful 8 Hz WBV. Moreover, extracellular signal-regulated kinase (ERK)-phosphorylation is most robust in neurons and astrocytes of the dorsal horn, with the most ERK phosphorylation occurring in the 8 Hz group. These findings indicate that a WBV exposure that induces persistent pain also induces a host of neuroimmune cellular activation responses that are also sustained. This work indicates there is an injury-dependent response that is based on the vibration parameters, providing a potentially useful platform for studying mechanisms of painful spinal injuries. © 2016 Orthopaedic Research Society. Published by Wiley Periodicals, Inc. *J Orthop Res* 34:1439–1446, 2016.

**Keywords:** vibration; pain; spine; lumbar; neuroinflammation

Low back pain can arise from many inciting events, including disc inflammation or herniation, inflammation or injury to the surrounding musculature, or nerve compression, among other pathologies.<sup>1–3</sup> There is extensive epidemiologic evidence pointing to exposure to whole-body vibration (WBV), especially at near-resonant low frequencies (4–10 Hz), as a leading risk factor for lower back disorders.<sup>4–7</sup> Helicopter pilots, in particular, are exposed to vibrations between 3 and 7 Hz,<sup>8</sup> and report increased back and neck pain incidents correlating to the length of the WBV-exposure.<sup>9</sup> Several epidemiological reviews have shown a strong relationship between human occupational WBV exposure near resonance at 4–6 Hz and likelihood of developing low back pain.<sup>10,11</sup> Although WBV-induced low back pain is common in both military<sup>8,9</sup> and civilian<sup>10,11</sup> populations, the underlying pathology and cellular mechanisms responsible for pain have only recently begun to be investigated.<sup>12–14</sup>

Neurons and glial cells in the spinal cord have potent roles in central sensitization and contribute to pain onset and maintenance.<sup>15–20</sup> After a painful injury, in addition to peripheral and central neuronal changes that decrease thresholds for activation and also increase activity in response to stimuli, immune cells become activated to lead to, and further maintain, neuronal responses in central sensitization.<sup>15,19,21</sup> Microglia, the resident macrophages of the brain and

spinal cord, are the first to respond, releasing a host of inflammatory mediators including cytokines, chemokines, and neurotrophins, which further activate additional microglia and astrocytes, and increase endothelial permeability allowing macrophages and monocytes to infiltrate the central nervous system (CNS).<sup>15–17,19,20,22</sup> In cases of chronic pain, central sensitization is established, with neuronal hyperexcitability, reduced firing thresholds, and unchecked feedback loops between glia and pro-inflammatory molecules even after the painful stimulus has been removed.<sup>15,17,18,23,24</sup> In fact, in rat models of pain from lumbar root constriction and/or inflammation, tissue injury has been linked to spinal glial activation and pain.<sup>15,20,25–29</sup> Similarly, in lumbar disc herniation models, there is a robust upregulation of spinal microglia and astrocytes corresponding to times when pain is evident.<sup>30</sup>

The inflammatory cascade after injury that leads to pain is induced first by microglia and macrophages, and later sustained by astrocytes with their modulatory effect on neurons.<sup>20,21,31,32</sup> This neuroimmune response activates a signaling cascade through the mitogen-activated protein kinase (MAPK)-pathway that is also thought to play a role in both the development, and ongoing maintenance of pain.<sup>16,29,33</sup> Extracellular signal-regulated kinases (ERKs), a subfamily of MAPKs that are activated via phosphorylation,<sup>34</sup> play a critical role in how cells respond to extracellular signals. In the superficial dorsal horn of the spinal cord where afferent fibers that transmit nociceptive signals synapse, ERK phosphorylation is associated with both painful stimuli and tissue damage.<sup>29,35–38</sup> Although previous work has shown glial activation in the cervical spinal cord only after WBV that induces sustained forepaw mechanical

Conflicts of interest: The authors have no additional professional or financial disclosures.

Grant sponsor: Department of Defense; Grant number: W81XWH-10-2-0140.

Correspondence to: Beth A. Winkelstein (T: 215-573-4589; F: 215-573-2071; E-mail: winkelst@seas.upenn.edu)

© 2016 Orthopaedic Research Society. Published by Wiley Periodicals, Inc.

sensitivity,<sup>14</sup> it is not known if painful WBV induces spinal ERK phosphorylation, and if so, in which cells.

We have previously shown that WBV induces mechanical allodynia, which can be taken as a proxy for pain, in the rat with temporal patterns that depend on the number of exposures, and the exposure profile of vibration.<sup>14,39</sup> In addition, activation of astrocytes and microglia in the cervical spinal cord has been shown to correlate with both the mechanical severity of the WBV exposure, and the magnitude and length of the pain response.<sup>14</sup> Previous work using a single exposure of WBV has shown that significant spinal compression is induced during WBV, along with transient pain in the hind paws.<sup>39</sup> Although whole-body vibration at 8 Hz induces more mechanical deformation and produces more robust immune activation in the cervical spinal cord and pain in the forepaws than does 15 Hz,<sup>14</sup> the effect of WBV at 8 Hz on the cellular and biochemical processes in the lumbar spinal cord is not known, nor is its relationship to WBV exposure parameters. Based on the fact that neuronal and glial activation in the spinal cord are pivotal in the development of persistent pain,<sup>16,21,31</sup> it is hypothesized that robust changes in glial activation and the ERK signaling pathway are likely in the lumbar spinal cord in association with the development and/or maintenance of pain.

## METHODS

All procedures were approved by the Institutional Animal Care and Use Committee at the University of Pennsylvania and performed in accordance with the recommendations of the International Association for the Study of Pain Committee for Research and Ethical Issues.<sup>40</sup> Experiments were performed using male Holtzman rats (Envigo, Indianapolis, IN) weighing  $313 \pm 15$  g at the start of the study, that were doubly housed according to those conditions recommended by the Association for Assessment and Accreditation of Laboratory Animal Care International with a 12/12 h light/dark cycle, environmental enrichment, and free access to food and water.

Rats were exposed to whole-body vibration (WBV) under isoflurane inhalation anesthesia (4% induction, 2% maintenance). Separate groups of randomly assigned rats underwent vibration at 8 Hz with 5 mm stroke ( $n = 6$ ) or 15 Hz with 1.5 mm stroke ( $n = 6$ ) for 30 min on each of days 0 and 7.<sup>14,39</sup> A third group of sham control rats ( $n = 6$ ) received only an anesthesia exposure under the same paradigm, and was not vibrated.<sup>13,14,39</sup> For all exposures, rats were placed on a shaker plate in the prone position with a nosecone delivering anesthesia, and were secured with straps under the shoulders and above the hips, as previously described.<sup>14,39</sup> Vibration was applied as a sinusoidal input at either of the designated conditions in the direction along the long-axis of the rat's spine using the shaker (Model K2007E01; The Modal Shop, Cincinnati, OH).

Behavioral sensitivity was assessed by measuring the withdrawal threshold in the bilateral hind paws in response to a mechanical stimulation, using conventional techniques.<sup>39,41</sup> Testing for behavioral sensitivity was performed before any WBV exposure (day 0) to provide baseline responses, and on days 1, 3, 5, 7, 9, 11, 13, and 14 to capture

a full week after each of the WBV exposures; behavioral sensitivity was assessed prior to the WBV exposure on day 7. Calibrated von Frey filaments ranging from 0.6 to 26 g (Model 58011; Stoelting, Wood Dale, IL) were used to stimulate the hind paw between the foot pads until the rat exhibited a positive response of lifting or licking the paw; any response was confirmed if a similar positive response was also evoked by the next highest filament strength.<sup>41</sup> On each day of assessment, rats were acclimated to the testing environment and tester for at least 15 min, followed by three rounds of testing with 10 min of rest between each round. Since the application of WBV is symmetric across the spine,<sup>13,14,39</sup> the responses of the left and right hind paws were averaged on each test day for each rat; a repeated-measures ANOVA with Tukey post hoc test compared the average withdrawal thresholds between the groups receiving 8 Hz, 15 Hz, or sham WBV.

On day 14, after behavioral testing, the lumbar spinal cord was harvested for immunohistochemical analyses of inflammatory cell activation and phosphorylated-ERK (p-ERK). Spinal cord from naïve rats ( $n = 2$ ) that were not exposed to vibration or anesthesia was also included as a normal control for all spinal cord assessments, and all animals were used for analyses (18/18 rats). Rats were anesthetized with sodium pentobarbital (65 mg/kg) and then perfused with 200 ml of ice-cold phosphate-buffered saline (PBS), followed by 200 ml of 4% paraformaldehyde (PFA) in PBS. Following euthanization, the lumbar enlargement (L2–L5) was removed en bloc and post-fixed overnight at 4°C in 4% PFA in PBS, followed by a week of cryoprotection at 4°C in 30% sucrose in PBS.<sup>13,14</sup> The enlargement was embedded in optimal cutting temperature compound and sectioned in the transverse plane (14  $\mu$ m thick sections) at L3. This sectioning protocol ensured that all immunolabeled sections were collected and compared at the same spinal level across all rats and groups.

Sections of lumbar spinal cord were co-labeled to evaluate immune cell activation and cell-specific p-ERK expression. Slides were rinsed in water, blocked in 10% goat serum in PBS with 0.3% Triton X-100, and incubated in primary antibodies to glial fibrillary acidic protein (GFAP), a structural component expressed in astrocytes, ionized calcium-binding adapter molecule 1 (IBA1), a protein upregulated during inflammation in microglia and macrophages, Neuronal Nuclei (NeuN), which labels the nucleus of all neurons, and p-ERK overnight at 4°C. Primary antibody dilutions were optimized for each antibody: GFAP (1:500, mouse, MAB360; Millipore, Billerica, MA), IBA1 (1:1000, rabbit, #019-19741; Wako, Osaka, Japan), NeuN (1:1000, conjugated to Alexa555, MAB377A5; Millipore), and p-ERK (1:500, conjugated to Alexa488, #4344; Cell Signaling, Danvers, MA). Sections were rinsed with PBS, incubated for 2 h at room temperature in goat anti-rabbit Marina Blue, and goat anti-mouse Alexa633 secondary antibodies (1:1000, Life Technologies, Carlsbad, CA), rinsed again in PBS, and coverslipped with antifade media. After drying, slides were imaged using a Zeiss Axioplan 2 microscope (Zeiss, Thornwood, NY) with each of the four labeled channels (350, 488, 555, and 633 nm) at 200 $\times$  magnification.

Images from each section (3–6 sections per rat) were captured using a Zeiss AxioCam HRm imaging system (Zeiss, Thornwood, NY) and cropped (750 pixels  $\times$  200 pixels) to contain the superficial (I and II) laminae of the dorsal horn.<sup>24,42</sup> Custom automated Matlab scripts (Matlab v7; Mathworks, Natick, MA) were used to set the thresholds for

fluorescent labeling based on the intensity ranges for positive pixels and background in normal naive tissue. The number of pixels positive for GFAP, IBA1, or p-ERK labeling was calculated as a percent of the total dorsal horn area that was evaluated. Total levels of each of GFAP, IBA1, and p-ERK labeling was then compared to the levels of each in the normal rats and expressed as fold-change over normal levels. Differences in normalized intensity were compared with separate one-way ANOVAs with Tukey post hoc analysis for each label and group.

In addition, in order to determine p-ERK expression patterns, analyses were performed to measure relative expression between cell-types and within each cell type. The distribution of p-ERK expression between each cell type in each group was determined by calculating the percent-pixels that were positive for both p-ERK and each of NeuN, GFAP, and IBA1 and dividing that by the total number of pixels that were positive for p-ERK labeling.<sup>14,43</sup> In order to compare the amount of p-ERK that was present in each cell type following the different WBV exposures, the pixels that were positive for p-ERK and either GFAP, IBA1, or NeuN were quantified and divided by the total number of pixels positive for each of GFAP, IBA1, or NeuN, respectively. These co-labeling values were compared between groups using separate one-way ANOVAs with Tukey post hoc analysis for each label and group.

## RESULTS

These WBV exposures produced significantly different behavioral sensitivity responses in the hind paw, with each group (8 Hz, 15 Hz, and sham) different from each other ( $p < 0.0001$ ). Sensitivity in the hind paw was induced as early as 1 day after an exposure to WBV at either 8 Hz ( $p < 0.0011$ ) or 15 Hz ( $p < 0.0273$ ) relative to their respective baseline responses and also relative to sham responses at day 1 ( $p < 0.0001$ ) (Fig. 1). On all days tested, the hind paw withdrawal threshold was significantly lower in the 8 Hz group compared to its corresponding baseline levels ( $p < 0.0011$ ) and also compared to sham withdrawal thresholds ( $p < 0.0001$ ) (Fig. 1). However, after a 15 Hz WBV, the threshold was only lower than its own baseline threshold on days 1, 3, and 5 ( $p < 0.0273$ ); it was lower than sham levels on all test days ( $p < 0.0110$ ), except day 14. Moreover, on day 14 after 8 Hz WBV, the withdrawal threshold was significantly lower than withdrawal thresholds for both sham ( $p < 0.0001$ ) and 15 Hz WBV ( $p < 0.0001$ ) (Fig. 1).

Paralleling the behavioral findings, labeling for both the astrocytic marker GFAP and the microglial and macrophage marker IBA1 was increased at day 14 only for the 8 Hz group (Fig. 2). There was significantly more GFAP labeling in the superficial dorsal horn of the 8 Hz group compared to levels evident in both the 15 Hz ( $p < 0.0048$ ) and sham ( $p < 0.0001$ ) groups (Fig. 2a). However, IBA1 labeling after the 8 Hz exposure was only significantly greater than sham levels ( $p < 0.0367$ ) (Fig. 2b). In fact, IBA1 expression in the 8 and 15 Hz groups was not significantly different from each other.

Similar to GFAP expression patterns, there was more phosphorylated ERK evident in the 8 Hz group

compared to both the 15 Hz ( $p < 0.0001$ ) and the sham ( $p < 0.0001$ ) groups, with no difference between those two groups (Fig. 3). Examining the distribution of p-ERK by cell-type assayed, no significant differences were detected in the amount of NeuN, GFAP, or IBA1 co-localized with p-ERK between any of the groups (Fig. 4). However, for all of the groups, there was significantly more NeuN co-localized with p-ERK than IBA1 co-localized with p-ERK ( $p < 0.0001$ ) (Fig. 4). Additionally, in the 8 Hz group, there was more GFAP than IBA1 co-localized with p-ERK ( $p < 0.0006$ ) (Fig. 4).

The amount of p-ERK expressed by each cell-type at day 14 in the superficial dorsal horn of the lumbar spinal cord after the different exposures exhibited different patterns (Fig. 5). Over 20% of the area labeled by the neuronal marker NeuN contained p-ERK ( $22.1 \pm 13.7\%$ ) in the 8 Hz group, which was significantly more neuronal expression than in the 15 Hz ( $8.3 \pm 17.5\%$ ,  $p < 0.0022$ ) or sham ( $4.8 \pm 8.5\%$ ,  $p < 0.0108$ ) groups (Fig. 5a). Similarly, there was also significantly more phosphorylated ERK in astrocytes after a painful 8 Hz exposure ( $41.0 \pm 25.4\%$ ) compared to that after a 15 Hz ( $30.2 \pm 17.6\%$ ,  $p < 0.0048$ ) and a sham ( $30.0 \pm 18.9\%$ ,  $p < 0.0001$ ) (Fig. 5b) exposure. In contrast, IBA1-positive cells (Fig. 5c), mainly microglia and macrophages, contained the most p-ERK as a percentage of their total labeled area, with more than 60% in each group (Fig. 5c). However, there were no differences in p-ERK between groups.

## DISCUSSION

Although WBV has long-been associated with neck and low back pain in epidemiological studies,<sup>4-7,10,11</sup> this is the first study linking WBV, pain, and molecu-

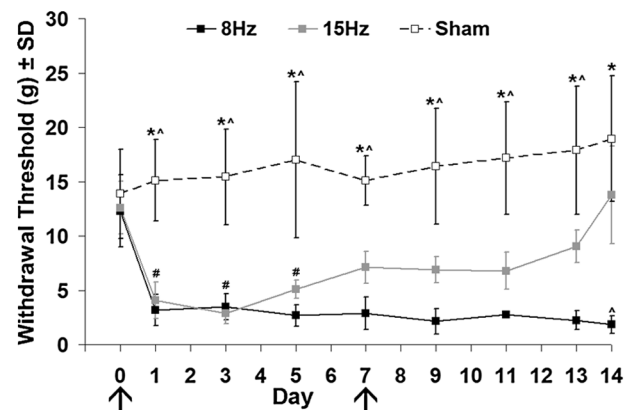


**Figure 1.** The hind paw withdrawal thresholds for 8 Hz, 15 Hz, and sham groups exhibit overall different patterns from each other ( $p < 0.0001$ ), despite having no difference at baseline (day 0). Exposure to WBV at 8 Hz induces a significant decrease in hind paw withdrawal threshold compared to baseline ( $p < 0.0011$ ) and sham ( $p < 0.0001$ ) on each day. A 15 Hz exposure produces only transient reductions from baseline on days 1, 3, and 5 ( $p < 0.0273$ ), but is significantly less than sham on days 1–13 ( $p < 0.0110$ ). However, only the 8 Hz exposure remains significantly decreased from baseline and sham through day 14, and is also significantly less than 15 Hz on day 14 ( $p < 0.0110$ ). Arrows indicate days of WBV exposure.

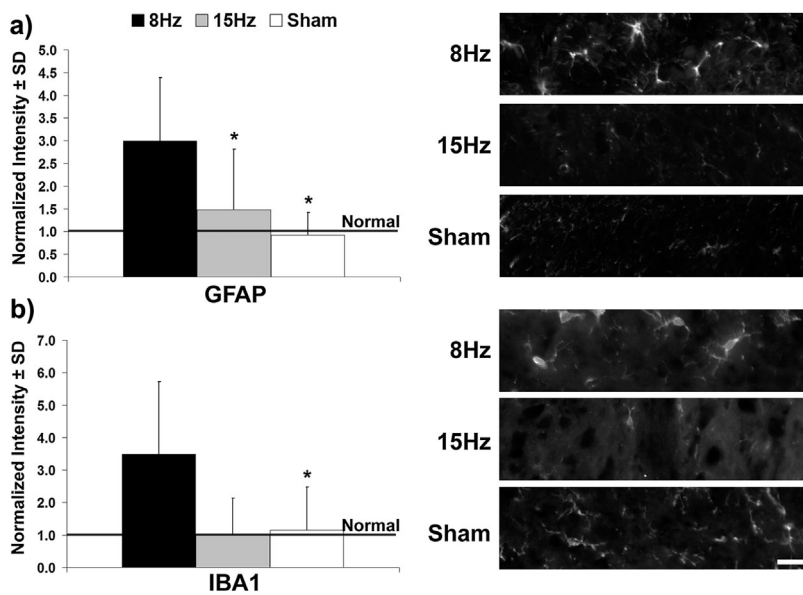


**Figure 2.** Quantification and representative images of inflammatory cell labeling in the superficial laminae of the dorsal horn in the lumbar spinal cord at day 14, expressed as fold-change over normal. GFAP (a), a marker of astrocytes, is significantly upregulated following WBV at 8 Hz ( $*p < 0.0048$ ) compared to 15 Hz and sham exposures. Similarly, following 8 Hz exposure, levels of IBA1 (b), a marker of microglia and macrophages, are also robustly increased compared to the response of a sham exposure ( $*p < 0.0367$ ). There is no difference in IBA1 labeling between the two WBV groups. The scale bar is 20  $\mu$ m and applies to all panels.

lar outcomes in the lumbar spinal cord (Figs. 1–5). Only following WBV that *also* induces sustained pain (8 Hz) are immune cells activated (Figs. 1 and 2); a similar response is also evident in the cervical spinal cord, in which microglia and astrocytes are both activated at a later time only following painful 8 Hz WBV.<sup>14</sup> Moreover, although MAPK signaling has been shown to increase, namely measured by levels of ERK phosphorylation, in models of low back and other chronic pain conditions,<sup>29,33,35,37,38,44</sup> this is the first study to demonstrate that this pathway is activated in several cell-types, but not microglia, in the superficial dorsal horn of the lumbar spinal cord following painful WBV (Figs. 4–6). The increase in p-ERK that is evident only in the neurons and astrocytes of the 8 Hz group (Fig. 5) parallels the increase in glial activation in the dorsal horn, as well as the pain response at day 14 (Figs. 1 and 2). These cell-specific increases in p-ERK levels, in coordination with overall increased glial activation, occur only in the case of sustained pain in the 8 Hz WBV group, suggesting there may be increased cross-talk between spinal neurons, specifically activated nociceptive neurons, and the inflammatory support cells surrounding them in the dorsal horn, which may contribute to pain maintenance, specifically through the MAPK pathway. However, since the NeuN label used in our study binds to all

neuronal nuclei, further studies are needed to determine which sub-populations, if any, are most active.

Behavioral sensitivity is induced as early as day 1 in the hind paws following both of the WBV exposures, but only the 8 Hz WBV produces long-lasting sustained allodynia through day 14 (Fig. 1). This exposure-dependent establishment of persistent pain following 8 Hz WBV suggests that different exposure parameters, such as the vibration frequency, displacement, and acceleration, may contribute to different local tissue responses, or even injury, which may drive pain. Interestingly, although the muscle response during exposure is absent due to anesthesia effects, pain develops early on after exposure. The transient, recovering allodynia that is observed here is consistent with a prior report with the same 15 Hz WBV exposures.<sup>39</sup> In contrast, a repeated daily exposure of 15 Hz WBV for 7 consecutive days did induce sustained sensitivity in the hind paw as well as increased neurotrophin expression in the intervertebral discs at day 14.<sup>13,39</sup> Interestingly, the 8 Hz WBV exposure only on days 0 and 7 is sufficient to induce sustained sensitivity lasting just as long (Fig. 1).<sup>14</sup> The behavioral findings suggest that the frequency and displacement of WBV, as well as the number of exposures, play roles in the nature of the pain response that develops. These experimental findings are aligned with epidemiological

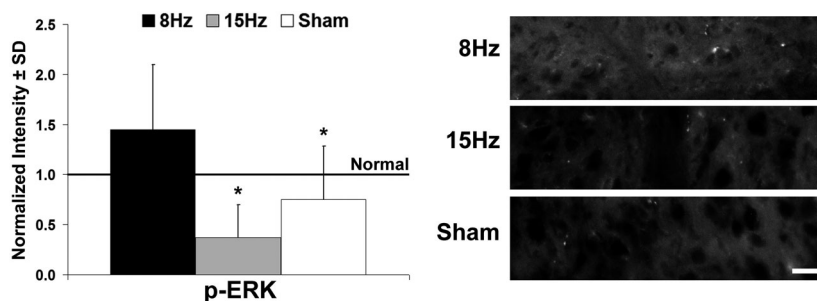


**Figure 3.** ERK phosphorylation in the superficial lumbar dorsal horn on day 14, expressed as fold-change over normal, is significantly higher following 8 Hz WBV than after 15 Hz WBV and sham ( $*p < 0.0001$ ). There is no difference in p-ERK levels between 15 Hz and sham. The scale bar is 20  $\mu$ m and applies to all images.

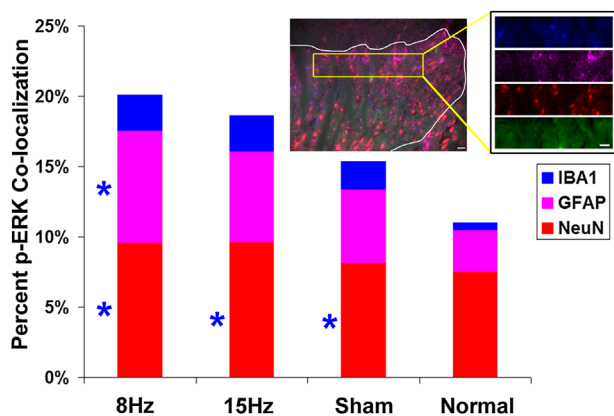


**Figure 4.** Quantification of the distribution of p-ERK labeling in the superficial dorsal horn of the lumbar spinal cord at day 14. Although the distribution of p-ERK between cell-types is not different between groups, in all groups there is significantly more NeuN (red) co-localized with p-ERK compared with that co-localized with IBA1 (blue) ( $*p < 0.0001$ ). Additionally, in the 8 Hz group, there is also significantly more p-ERK in the GFAP-positive areas (magenta) compared to that with IBA1-positive areas ( $*p < 0.0006$ ). The representative image shows the dorsal horn after 8 Hz WBV with labeling for IBA1 (blue), GFAP (magenta), NeuN (red), and p-ERK (green). Both scale bars are 20  $\mu$ m.

studies reporting an association between the *length* of WBV exposure and the duration and/or severity of low back pain symptoms.<sup>9,45,46</sup> However, it is important to note that only two WBV frequencies were assessed in our study; it has been shown that the resonance of the spine varies with species and that the human may exhibit a more complex resonance response.<sup>12,47,48</sup> Although many factors affect the resonance of the spine, under the conditions used here, the rat's thoracic spine exhibits a maximum transmissibility at 8 Hz.<sup>14</sup>

The hind paw sensitivity responses induced by both WBV exposures used in this study (Fig. 1) exhibit similar patterns in terms of duration and magnitude of the sensitivity that is induced in the forepaw,<sup>14,39</sup> suggesting that WBV likely induces injury along the full length of the spine. Although similarities are observed between the pain responses across spinal regions, the behavioral sensitivity has been measured in response to mechanical stimuli only, and thermal sensitivity has not been assayed in this model of vibration injury. Since, hot and/or cold sensitivity have been linked with immune activation in the spinal cord<sup>49</sup> and spinal hyperexcitability,<sup>23,24</sup> it would be important to also determine if WBV induces similar patterns of thermal sensitivity and if they exhibit any regional differences. Moreover, axial pain was not explicitly evaluated here and would provide additional context to this work, with assays of function also providing meaningful translation to the human low back pain condition.<sup>50</sup>

Sustained lumbar spinal glial activation is only evident following the 8 Hz WBV which induces sustained pain (Figs. 1 and 2). This is expected given that WBV at 8 Hz is both more painful (Fig. 1) and mechanically injurious than at 15 Hz.<sup>14</sup> The markers of astrocytic (GFAP) and microglial (IBA1) activation are only up-regulated at day 14 in the painful 8 Hz case, whereas the 15 Hz WBV exposure does not alter either the cellular response or exhibit pain at that same time point (Figs. 1, 2, and 5). However, spinal immune activation was only assayed at day 14 and given the differences in behavioral outcomes over time between the two WBV exposures, defining the early spinal responses would determine if differential pathways are activated between groups. This same pattern of glial activation evident after the 8 Hz

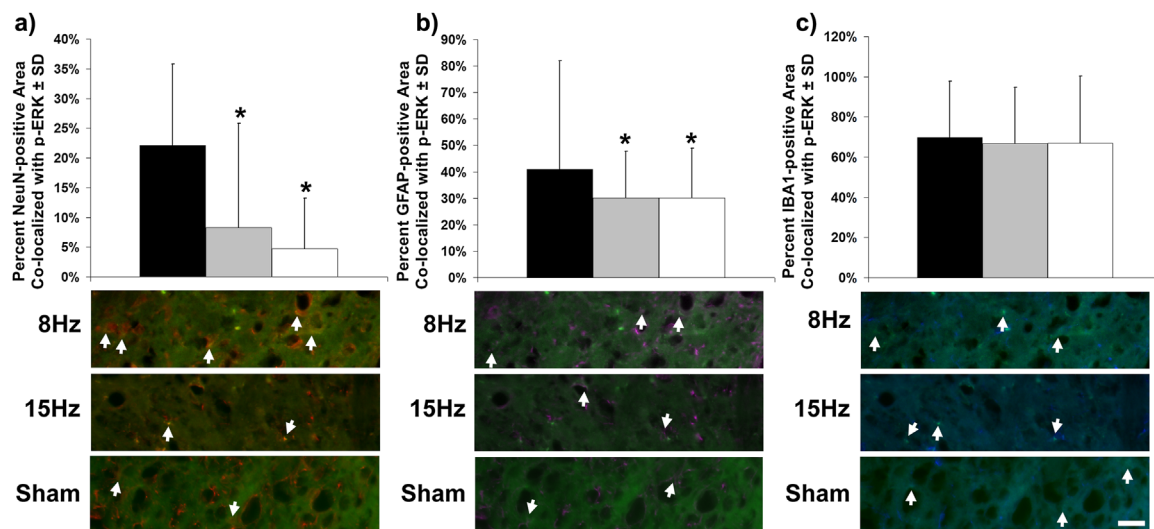


**Figure 5.** Quantification and representative images of the percent area of each cell label co-localized with p-ERK on day 14 in the lumbar superficial dorsal horn. There is significantly more p-ERK (green) in NeuN positive (red) areas (a), with robust ERK signaling in neurons (co-localization is yellow), for 8 Hz WBV compared to both 15 Hz and sham ( $*p < 0.0108$ ). Similarly, there is also significantly more p-ERK (green) in the GFAP-positive (magenta) areas (b) of the 8 Hz group compared to both 15 Hz and sham ( $*p < 0.0048$ ). Astrocytes co-localized (white) with p-ERK are indicated with arrows. In the IBA1-positive (blue) areas (c), there are no differences in p-ERK levels (green) between any groups. Arrows indicate co-labeling (bright green) of microglia/macrophages with p-ERK. The scale bar is 20  $\mu$ m and applies to all images.

exposure and not the 15 Hz WBV is similar to the findings in the cervical spinal cord for these same WBV conditions.<sup>14</sup> Interestingly, glial outcomes parallel behavior regardless of anatomical location—with both cervical and lumbar inflammation only in the sustained painful WBV instances (Figs. 1 and 2).<sup>14</sup> The association between chronic pain and glial activation in the spinal cord is well-established in a wide variety of different injury models, ranging from whiplash to nerve root compression to intervertebral disc injury.<sup>19,20,25–28,30,43,51</sup> However, GFAP expression in the lumbar spinal cord has been shown not to necessarily reflect the severity of neural tissue injury.<sup>20</sup> It should be noted that labeling of GFAP and IBA1 serve only as proxy measurements for glial activation. Additional studies evaluating other MAPKs, ERK isoforms,<sup>44</sup> and comparing the phosphorylated to total ERK in glia would further elucidate the role of those and other inflammatory cells in WBV-induced pain. Nevertheless, this assessment of p-ERK in these glial cells and neurons of the spinal cord has begun to establish there is not just an increase in glial cell number or size (Fig. 2), but also an increase in their cellular activation (Figs. 4 and 5).

Activation of the MAPK signaling pathway, measured here by ERK phosphorylation, in the lumbar superficial dorsal horn on day 14 appears to occur *only* following the painful 8 Hz WBV (Figs. 3–5). ERK activation is known to play a role in neuronal plasticity and central sensitization,<sup>18,33,52,53</sup> and upregulation of p-ERK has been reported in the dorsal horn following injury and noxious stimuli.<sup>29,35,37,52,53</sup> Indeed, our study found a greater fraction of p-ERK in dorsal horn neurons than in microglia in all groups, regardless of the presence of sustained pain or not (Fig. 4). This differential response may be attributed to the relative workload and size of these cell types—glia play more of a supportive role while neurons are constitutively active. Interestingly, p-ERK levels in neurons in the spinal cord peak as early as 10 min after a painful spinal nerve ligation, and decrease by 6 h but are still evident.<sup>38</sup> As such, it is possible that neuronal p-ERK may be even more robust at earlier times following WBV. The 8 Hz group has the most p-ERK in NeuN-positive areas (Fig. 5a), which has been suggested as a more sensitive marker of neuronal activation and plasticity in central sensitization than c-Fos.<sup>18</sup> In addition to neuronal p-ERK, there is a larger proportion of GFAP-positive p-ERK compared to IBA1-positive areas only in the painful 8 Hz WBV group on day 14 (Fig. 4). That finding suggests that MAPK signaling in astrocytes may play a role in the maintenance of WBV-induced pain (Fig. 1); whereas, the ERK pathway does not seem to be active in microglia (Figs. 4 and 5). It also suggests p-ERK in astrocytes may be a sensitive marker of pain-related activation, similar to p-ERK in neurons,<sup>18,37,38,44</sup> and further supports the importance of glial activity in pain onset and maintenance.

This tunable model of non-surgical sub-catastrophic spinal injury with direct relevance to the injury environment for low back pain provides a platform to study the effects of WBV on pain—relating nociceptive, physiologic and biomechanical mechanisms in all spinal regions. The cervical and lumbar neuroinflammation that is observed following WBV recapitulates the cascades that are active at early and later time points in chronic pain,<sup>22</sup> including increased production of cytokines/chemokines, activation of astrocytes and microglia (Fig. 2), and robust signaling of PKC $\epsilon$ /p-ERK indicative of cellular activation (Figs. 3–5).<sup>14</sup> Of these responses, the p-ERK/MAPK signaling pathway is gaining increased attention as a potential target for treating inflammatory and neuropathic pain.<sup>22,36–38</sup> Given that similar signaling pathways are activated following WBV and a host of other highly prevalent, difficult to treat, painful neck and low back injuries,<sup>2,3,16–20,26–28,31</sup> the findings of the current study indicate even single and potentially subtle injury exposures, like WBV, can have sustained effects on central sensitization and pain.

#### AUTHORS' CONTRIBUTIONS

All of the authors (MEZ, SK, BAW) together designed the studies and contributed to the data analysis and interpretation, as well as the manuscript writing, editing, and final approval. MEZ and SK generated and processed all of the tissue analyzed for these experiments; MEZ performed the data analysis and with BAW interpreted and integrated the findings, as well as drafted and revised the manuscript.

#### REFERENCES

1. Deyo RA. 1998. Low-back pain. *Sci Am* 279:48–53.
2. Hooten WM, Cohen SP. 2015. Evaluation and treatment of low back pain: a clinically focused review for primary care specialists. *Mayo Clin Proc* 90:1699–1718.
3. Patrick N, Emanski E, Knaub MA. 2016. Acute and chronic low back pain. *Med Clin North Am* 100:169–181.
4. Blood RP, Yost MG, Camp JE, et al. 2015. Whole-body vibration exposure intervention among professional bus and truck drivers: a laboratory evaluation of seat-suspension designs. *J Occup Environ Hyg* 12:351–362.
5. Bovenzi M. 2009. Metrics of whole-body vibration and exposure-response relationship for low back pain in professional drivers: a prospective cohort study. *Int Arch Occup Environ Health* 82:893–917.
6. Magnusson ML, Pope MH, Wilder DG, et al. 1996. Are occupational drivers at an increased risk for developing musculoskeletal disorders? *Spine* 21:710–717.
7. Torén A, Oberg K, Lembke B, et al. 2002. Tractor-driving hours and their relation to self-reported low-back and hip symptoms. *Appl Ergon* 33:139–146.
8. De Oliveira CG, Nadal J. 2005. Transmissibility of helicopter vibration in the spines of pilots in flight. *Aviat Space Environ Med* 76:576–580.
9. Nevin RL, Means GE. 2009. Pain and discomfort in deployed helicopter aviators wearing body armor. *Aviat Space Environ Med* 80:807–810.
10. Bovenzi M, Hulshof CT. 1999. An updated review of epidemiologic studies on the relationship between exposure to whole-body vibration and low back pain (1986–1997). *Int Arch Occup Environ Health* 72:351–365.

11. Milosavljevic S, Bagheri N, Vasiljev RM, et al. 2011. Does daily exposure to whole-body vibration and mechanical shock relate to the prevalence of low back and neck pain in a rural workforce? *Ann Occup Hyg* 56:10–17.
12. Baig HA, Dorman DB, Bulka BA, et al. 2014. Characterization of the frequency and muscle responses of the lumbar and thoracic spines of seated volunteers during sinusoidal whole body vibration. *J Biomech Eng* 136:101002.
13. Kartha S, Zeeman ME, Baig HA, et al. 2014. Upregulation of BDNF and NGF in cervical intervertebral discs exposed to painful whole-body vibration. *Spine* 36:1542–1548.
14. Zeeman ME, Kartha S, Jaumard NV, et al. 2014. Whole-body vibration at thoracic resonance induces sustained pain and widespread cervical neuroinflammation in the rat. *Clin Orthop Relat Res* 473:2936–2947.
15. DeLeo JA, Winkelstein BA. 2002. Physiology of chronic spinal pain syndromes: from animal models to biomechanics. *Spine* 27:2526–2537.
16. DeLeo JA, Tanga FY, Tawfik VL. 2004. Neuroimmune activation and neuroinflammation in chronic pain and opioid tolerance/hyperalgesia. *Neuroscientist* 10:40–52.
17. Gao YJ, Ji RR. 2010. Chemokines, neuronal-glia interactions, and central processing of neuropathic pain. *Pharmacol Ther* 126:56–68.
18. Latremoliere A, Woolf CJ. 2009. Central sensitization: a generator of pain hypersensitivity by central neural plasticity. *J Pain* 10:895–926.
19. Watkins LR, Milligan ED, Maier SF. 2001. Glial activation: a driving force for pathological pain. *Trends Neurosci* 24: 450–455.
20. Winkelstein BA, DeLeo JA. 2002. Nerve root injury severity differentially modulates spinal glial activation in a rat lumbar radiculopathy model: considerations for persistent pain. *Brain Res* 956:294–301.
21. DeLeo JA, Yeziarski RP. 2001. The role of neuroinflammation and neuroimmune activation in persistent pain. *Pain* 90:1–6.
22. Ji RR, Xu ZZ, Gao YJ. 2014. Emerging targets in neuroinflammation-driven chronic pain. *Nat Rev Drug Discov* 13:533–548.
23. Kras JV, Weisshaar CL, Pall PS, et al. 2015. Pain from intra-articular NGF or joint injury in the rat requires contributions from peptidergic joint afferents. *Neurosci Lett* 604:193–198.
24. Nicholson KJ, Zhang S, Gilliland TM, et al. 2014. Riluzole effects on behavioral sensitivity and the development of axonal damage and spinal modifications that occur after painful nerve root compression. *J Neurosurg Spine* 20: 751–762.
25. Cao H, Zhang YQ. 2008. Spinal glial activation contributes to pathological pain states. *Neurosci Biobehav Rev* 32: pageFirst>972–983.
26. Colburn RW, Rickman AJ, DeLeo JA. 1999. The effect of site and type of nerve injury on spinal glial activation and neuropathic pain behavior. *Exp Neurol* 157:289–304.
27. Garrison CJ, Dougherty PM, Kajander KC, et al. 1991. Staining of glial fibrillary acidic protein (GFAP) in lumbar spinal cord increases following a sciatic nerve constriction injury. *Brain Res* 565:1–7.
28. Hashizume H, DeLeo JA, Colburn RW, et al. 2000. Spinal glial activation and cytokine expression after lumbar root injury in the rat. *Spine* 25:1206–1217.
29. Ji RR, Baba H, Brenner GJ, et al. 1999. Nociceptive-specific activation of ERK in spinal neurons contributes to pain hypersensitivity. *Nat Neurosci* 2:1114–1119.
30. Miyagi M, Ishikawa T, Orita S, et al. 2011. Disk injury in rats produces persistent increases in pain-related neuropeptides in dorsal root ganglia and spinal cord glia but only transient increases in inflammatory mediators: pathomechanism of chronic diskogenic low back pain. *Spine* 36: 2260–2266.
31. Stafford MA, Peng P, Hill DA. 2007. Sciatica: a review of history, epidemiology, pathogenesis, and the role of epidural steroid injection in management. *Br J Anaesth* 99:461–473.
32. Strong JA, Xie W, Bataille FJ, et al. 2013. Preclinical studies of low back pain. *Mol Pain* 9:17.
33. Ji RR, Gereau RW 4th, Malcangio M, et al. 2009. MAP kinase and pain. *Brain Res Rev* 60:135–148.
34. Thomas KL, Hunt SP. 1993. The regional distribution of extracellularly regulated kinase-1 and -2 messenger RNA in the adult rat central nervous system. *Neuroscience* 56: 741–757.
35. Karim F, Wang CC, Gereau RW 4th. 2001. Metabotropic glutamate receptor subtypes 1 and 5 are activators of extracellular signal-regulated kinase signaling required for inflammatory pain in mice. *J Neurosci* 21:3771–3779.
36. Kras JV, Weisshaar CL, Quindlen J, et al. 2013. Brain-derived neurotrophic factor is upregulated in the cervical dorsal root ganglia and spinal cord and contributes to the maintenance of pain from facet joint injury in the rat. *J Neurosci Res* 91:1312–1321.
37. Ma W, Quirion R. 2005. The ERK/MAPK pathway, as a target for the treatment of neuropathic pain. *Expert Opin Ther Targets* 9:699–713.
38. Zhuang ZY, Gerner P, Woolf CJ, et al. 2005. ERK is sequentially activated in neurons, microglia, and astrocytes by spinal nerve ligation and contributes to mechanical allodynia in this neuropathic pain model. *Pain* 114:149–159.
39. Baig HA, Guarino BB, Lipschutz D, et al. 2013. Whole body vibration induces forepaw and hind paw behavioral sensitivity in the rat. *J Orthop Res* 31:1739–1744.
40. Zimmerman M. 1983. Ethical guidelines for investigations of experimental pain in conscious animals. *Pain* 16:109–110.
41. Chaplan SR, Bach FW, Pogrel JW, et al. 1994. Quantitative assessment of tactile allodynia in the rat paw. *J Neurosci Methods* 53:55–63.
42. Zhang S, Nicholson KJ, Smith JR, et al. 2013. The roles of mechanical compression and chemical irritation in regulating spinal neuronal signaling in painful cervical nerve root injury. *Stapp Car Crash J* 57:219–242.
43. Nicholson KJ, Guarino BB, Winkelstein BA. 2012. Transient nerve root compression load and duration differentially mediate behavioral sensitivity and associated spinal astrocyte activation and mGluR5 expression. *Neuroscience* 209: 187–195.
44. Obata K, Katsura H, Mizushima T, et al. 2007. Roles of extracellular signal-regulated protein kinases 5 in spinal microglia and primary sensory neurons for neuropathic pain. *J Neurochem* 102:1569–1584.
45. Pope MH, Magnusson M, Wilder DG. 1998. Low back pain and whole body vibration. *Clin Orthop Relat Res* 354:241–248.
46. Tiemessen IJ, Hulshof CT, Frings-Dresen MH. 2008. Low back pain in drivers exposed to whole body vibration: analysis of a dose-response pattern. *Occup Environ Med* 65:667–675.
47. Kitazaki S, Griffin MJ. 1998. Resonance behaviour of the seated human body and effects of posture. *J Biomech* 31: 143–149.
48. Panjabi MM, Andersson GB, Jorneus L, et al. 1986. In vivo measurements of spinal column vibrations. *J Bone Joint Surg Am* 68:695–702.
49. Shen Y, Zhang ZJ, Zhu MD, et al. 2015. Exogenous induction of HO-1 alleviates vincristine-induced neuropathic pain by reducing spinal glial activation in mice. *Neurobiol Dis* 79:100–110.

50. Millecamps M, Czerminski JT, Mathieu AP, et al. 2015. Behavioral signs of axial low back pain and motor impairment correlate with the severity of intervertebral disc degeneration in a mouse model. *Spine J* 15:2524–2537.
51. Dong L, Smith JR, Winkelstein BA. 2013. Ketorolac reduces spinal astrocytic activation and PAR1 expression associated with attenuation of pain after facet joint injury. *J Neurotrauma* 30:818–825.
52. Ji RR, Woolf CJ. 2001. Neuronal plasticity and signal transduction in nociceptive neurons: implications for the initiation and maintenance of pathological pain. *Neurobiol Dis* 8:1–10.
53. Wei F, Vadakkan KI, Toyoda H, et al. 2006. Calcium calmodulin-stimulated adenylyl cyclases contribute to activation of extracellular signal-regulated kinase in spinal dorsal horn neurons in adult rats and mice. *J Neurosci* 26:851–861.